Visual Servoing Based Synced Motion Control of an Eight Bar Parallel Manipulator

Author

ZUKHRAF JAMIL

00000170498

Supervisor

DR. WAQAR SHAHID QURESHI

DEPARTMENT OF MECHATRONICS ENGINEERING
COLLEGE OF ELECTRICAL & MECHANICAL ENGINEERING
NATIONAL UNIVERSITY OF SCIENCES AND TECHNOLOGY
ISLAMABAD
OCTOBER, 2019

Visual Servoing Based Synced Motion Control of an Eight Bar Parallel Manipulator

Author
ZUKHRAF JAMIL
00000170498

A thesis submitted in partial fulfillment of the requirements for the degree of

MS Mechatronics Engineering

Thesis Supervisor:
DR. WAQAR SHAHID QURESHI

Thesis Supervisor's Signature:_____

DEPARTMENT OF MECHTRONICS ENGINEERING
COLLEGE OF ELECTRICAL & MECHANICAL ENGINEERING
NATIONAL UNIVERSITY OF SCIENCES AND TECHNOLOGY, ISLAMABAD
OCTOBER, 2019

Declaration

I certify that this research work titled "*Visual Servoing Based Synced Motion Control of an Eight Bar Parallel Manipulator"* is my own work. The work has not been presented elsewhere for assessment. The material that has been used from other sources it has been properly acknowledged / referred.

ZUKHRAF JAMIL

2016-NUST-Ms-MTS16

Language Correctness Certificate

This thesis has been read by an English expert and is free of typing, syntax, semantic, grammatical and spelling mistakes. Thesis is also according to the format given by the university.

ZUKHRAF JAMIL

Signature of Supervisor

Copyright Statement

- Copyright in text of this thesis rests with the student author. Copies (by any process) either in full, or of extracts, may be made only in accordance with instructions given by the author and lodged in the Library of NUST College of E&ME. Details may be obtained by the Librarian. This page must form part of any such copies made. Further copies (by any process) may not be made without the permission (in writing) of the author.

- The ownership of any intellectual property rights which may be described in this thesis is vested in NUST College of E&ME, subject to any prior agreement to the contrary, and may not be made available for use by third parties without the written permission of the College of E&ME, which will prescribe the terms and conditions of any such agreement.

- Further information on the conditions under which disclosures and exploitation may take place is available from the Library of NUST College of E&ME, Rawalpindi.

Acknowledgements

All praise to Allah, there is no deity except Him. I give my love and acknowledgement to family and friends for their constant support to achieve another milestone in my life.

I offer my sincere gratitude to Dr. Waqar Shahid Qureshi for his kind supervision and support for this work.

Abstract

Recently, there has been a significant recognition of user centered designs for interactive robotic systems. These computer-based activity-promoting interactive systems have proven to be potential therapeutic tools for exercise, injury, postural, and vestibular rehabilitation and control. This research focuses on working of such a user centered interactive system. This aim of the study is to design a phase and frequency controller based on visual servoing for a parallel manipulator to synchronize its motion with the head of a user walking or running on a treadmill. The synced motion of the platform would then enable the user to comfortably view a screen that will seem stationary to the user while running on treadmill. The purpose is to minimize relative motion between its end-effector that holds the device, and face of running user. The research work is divided into three modules: image processing, mathematical modeling, and interfacing of both modules. The platform is controlled based on visual feedback from fixed camera for face of user, and feedback from robotic manipulator for position of end-effector. The presented mechanical design and control strategy are tested for different users running with distinct speeds. The results show that motion of end-effector is successfully synchronized with the face of user at required speeds. The control strategy works effectively for the proof of concept yet modifications are recommended for increased computational accuracy.

Key Words: *User centered design, parallel manipulator, Visual servoing, Visual feedback*

Table of Contents

CHAPTER 1: INTRODUCTION 1

1.1 Background 1

1.2 Motivation 3

1.3 Scope of Research 3

1.4 Thesis Layout 5

CHAPTER 2: HUMAN MOTION MODELING 8

2.1. Motion Tracking 9

2.1.1. Tracker Selection 9

2.1.2. Detection and Tracking 13

2.2. Trajectory Mapping 15

2.3. Trajectory Analysis 16

CHAPTER 3: SYSTEM DESIGN 23

3.1. Mathematical Modeling 23

3.2. Model Analysis 27

CHAPTER 4: CONTROLLER DESIGN 29

4.1 Vision Based Control: 29

CHAPTER 5: IMPLEMENTATION AND RESULTS 35

CHAPTER 6: CONCLUSION AND FUTURE WORK 39

REFERENCES 40

List of Figures

Figure 1: Basic control strategy for controller design to achieve synchronization between manipulator and user facing it 5

Figure 2: Head motion tracking and trajectory mapping algorithm 14

Figure 3: Experimental setup to capture head motion trajectory 17

Figure 4: GUI developed for offline trajectory analysis 18

Figure 5: Head motion trajectory mapped in sagittal plane at two walking velocities: 1.78 m/s and 2.68 m/s 19

Figure 6: Head motion trajectory mapped in sagittal plane at two running velocities: 3.57 m/s and 4.47 m/s 19

Figure 7: Comparison of head displacement and velocity in 2D sagittal plane while walking at speed of 2.68 m/s 20

Figure 8: Comparison of head displacement and velocity in 2D sagittal plane while running at speed of 4.47 m/s 21

Figure 9: (a) mechanical design of the geared eight bar mechanism (b) vector loop diagram of the system 24

Figure 10: Two vector loops for mathematical modeling 25

Figure 11: Comparison of manipulator trajectory through mathematical; modeling and geometry design 28

Figure 12: User-Platform interface design based on real-time video feedback obtained from stationary camera 31

Figure 13: Platform synchronization control 34

Figure 14: Experimental Setup: the platform is placed stationary in front of the user at a fixed distance from the treadmill 35

Figure 15: Comparison of frequency ratios at selected speeds 38

List of Tables

Table 1 The evaluated (a) center location error (b) area overlap ratio and (c) success rate of KCF tracker for different fps 12

Table 2 Experimental Dataset 17

Table 3 Average head velocities for walking and running at selected speeds..... 21

Table 4: Pseudo code for face detection and tracking to get maxima of user trajectory 32

Table 5: Pseudo code for synchronization of moving platform with user's head trajectory 32

Table 6 Success rate of prototype testing for users running at selected treadmill speeds 36

Table 7 Average frequency ratio obtained for motion synchronization at three selected speeds 37

CHAPTER 1: INTRODUCTION

1.1 Background

Advances in human motion recognition and analysis techniques are revolutionizing the concept of Human Computer Interaction (HCI) combining laws of machine vision and biomechanics. The interdisciplinary field of HCI has helped in overcoming challenges in the field of robotics, physical and cognitive rehabilitation, sports, entertainment and other automation fields that depend upon intuitive and natural human machine interface [1] [2] .

Human motion recognition and analysis has played a significant role in humanoid robot control that requires imitation of human motion. It has also key role in development of platforms for rehabilitation of gait, posture, gaze, and other cognitive and musculoskeletal disorders. Using human activity models, smarter and robust platforms are developed for assisting disabled and elderly people to improve their quality of life [3] . These rehabilitation platforms are also used for sports and entertainment as effective and enjoyable tools for training. Various clinical and home based training platforms are developed for gaze stabilization and vestibular rehabilitation [4] [5]. The patients are trained using dual tasks to improve postural balance and reduce dizziness to avoid falling during high velocity or rapid head movements. An area of research to address this issue focuses on use of biofeedback and self-paced/force platforms [6]for balance and other mobility disorders therapy studies. The systems usually include headsets and eye trackers for tracking human motion on the platform [7] [8].

These designs are developed to uniquely address a variety of topics of research for improved outcomes and show much promise of improved gait and gaze rehabilitation training. Yet, there

lies plausible anecdotal evidence that suggests that various commercially available off-the-shelf training solutions and platforms do not produce encouraging outcomes in terms of controlled and focused training required for effective outcome based therapy [9]. Some weighing user feedback even shows that these general commercial solutions are not suitable for stroke, spinal cord, and traumatic brain injury therapy. The systems provide negative feedback leading to misinformation for the patients who are performing fine [10]. This is mainly because the users cannot keep up to the system's pace for activity or game play or are unable to perform required tasks set by game.

Based on such challenges, there is rapid research going on the user-centered design of such rehabilitation and training platforms [11] [9]. User centered design is an iterative process based on user needs and feedback. The user-centered designs are made customizable to be used by a set of specific users having a range of ability levels. Treadmill training is one such example of user centered designs. There are variations of commercial and clinical treadmills [12] available for exercise and rehabilitation trainings. These treadmills are used for exercise at homes [13], by athletes for sports training, and for rehabilitation therapies of musculoskeletal disorders, vestibular disorders [14], stroke, and knee/spine surgery patients.

Where the treadmill platforms are helpful in carrying out the subsequent therapies effectively, treadmill walking and running has shown to have a negative effect on body posture in sagittal plane. The problem gets even severe for the individuals having gaze, balance impairments or other vestibular disorders.

1.2 Motivation

Recently, the embedding of LCD screens into treadmills have allowed for users to enjoy their own media while exercising. While this caters for individualization and positive exercise results [15], it affects vestibular balance and can lead to risk of fall by distracting users to look downward or upward instead of running upright. Even in case of adjustable but fixed LCDs, the user has increased chances of neck strain, excess pressure on eyes, dizziness, and nausea since proper concentration requires zero relative motion between viewer and the object.

An approach to eliminate the relative motion between the treadmill user and LCD is to synchronize the motion of the use and screen. Lin and Koichi [16] has proposed one such solution. Their research focuses on developing a platform proposed that can track a user's head motion to minimize motion slip between human head and computer screen by eliminating relative motion between the platform and user during rapid head motions [17] [18].

1.3 Scope of Research

This study aims to device the control strategy for the synchronization of motion between the user and platform. As the treadmill is usually for sagittal locomotion patterns, two cases of walking and running are considered based on gaze and gait stabilization requirements from literature review.

A general dynamics and control problem requires computation of control torque variables as output. This control scheme is commonly used for serial manipulators in which joint matrices are computed for the control of end effector pose. This control approach is applicable both for joint

space and Cartesian space. However, there lies little available literature on the analytical modeling of parallel robots through forward kinematics [19]. The main reason for that is the complexity of calculating joint matrices of parallel robots using forward kinematics. Unlike serial robots, calculating accurate pose of the end effector in a parallel platform is a challenging task. The system consists of various redundancies for which the solution can only be obtained via solving set of nonlinear equations iteratively. This leads to convergence complexities in solution. Hence, parallel robot control models are developed in Cartesian plane. One of the most suitable approach for developing these models in through the use of exteroceptive components. These include any additional mechanical component foo the pose estimation in the form of motion sensors, serial ports, or vision sensors. Among these models, this study focuses on the development of a control scheme based on a vision sensor for pose estimation. Vision sensors are off the shelf, low cost, and more accurate in terms of determining motion parameters to be used for high speed motion applications. Use of vision sensors also reduces computational cost as there is only one set of computation parameters is required for pose estimation in Cartesian plane only.

The novelty of the work lies in eliminating biofeedback; as the system takes visual input only, the reliance on bio contact sensors is also eliminated. It helps in making the design off-the-shelf that can be mounted on treadmill or any external support as it takes visual feedback only to control platform motion. Another aspect is to reduce computational complexity that would need lesser processing time and storage. Therefore, visual servoing is further simplified by keeping the image acquisition and processing in 2D only.

1.4 Thesis Layout

The preliminary literature review suggests that controller requirements depend greatly on the type of visual input and geometry of the robot. Considering the novelty of the design proposed the research work was divided into three stages:

1. Human head motion modeling and analysis
2. Robotic platform mathematical modeling
3. Controller design for the integration of the image acquisition and platform motion modules.

The three modules are illustrated in Figure 1 and a brief summary of each module is describe below.

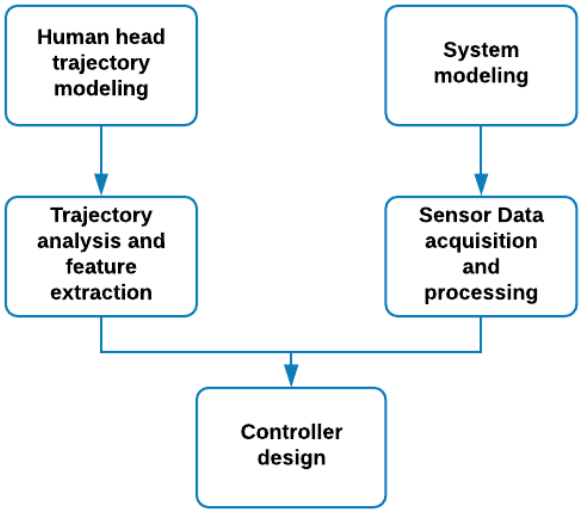

Figure 1: Basic control strategy for controller design to achieve synchronization between manipulator and user facing it

Human Head Motion Modeling:

The purpose of the study is to devise a mechanism that allows a user to comfortably view a screen placed in front of treadmill; the first research question sets as to what trajectory human head traces in sagittal plane while in forward locomotion (walking and running). Hence, modeling that trajectory was set the baseline criteria for further progress. Chapter 2 describes the approach followed for developing generalized trajectory models for these locomotion patterns and their kinematic analysis based on feature extraction. The choice between point to point detection and tracking is explained and selection criteria is discussed in detail as the feature extraction and mapping would play a significant role in accurate data acquisitions.

System Modeling:

Once successfully developed and validated, the generalized head motion model sets the requirements to what kind of manipulator should be selected that can trace the trajectory similar to head motion in 2D plane. Chapter 3 deals with the review of the robotic designs currently available (both series and parallel) and their limitations for the operation and control in this study. A novel parallel manipulator designed for the purpose of this study is explained and modeled for control purposes.

Controller Design:

The control strategy is selected considering the nature of features extracted, geometry of the manipulator, and accuracy requirements for synchronization. Chapter 4 discusses the control law adopted for the motion synchronization between the user and platform. The interfacing of all

three modules is discussed in detailed. The subsequent chapters elaborate the implementation and testing procedure and results obtained.

CHAPTER 2: HUMAN MOTION MODELING

Human motion models developed using visual or depth cues are utilized for action and activity recognition in all contemporary academic, medical and industrial robotic applications. Some promising applications include smart surveillance, medical and physiotherapy, sports, and gaming fitness training [17-18], and other applications for assistive and proactive services involving human-computer interaction [20-21]. These and a variety of other applications require different human motion models based on user interaction with the computer. The interaction may require hand motion, face, or gesture recognition in some interactive applications while other may rely on leg/limb, center of mass, and head notion models for various type of activity recognition.

Currently, the aforementioned studies for human motion modeling have focused on full body models, leg/limb, or trunk movements to develop generalized locomotion models. This requires capturing full body from side or from both front and side and therefore increases equipment complexity. On the other hand, generalized locomotion trajectories (such as for walking, running, hopping) can also be modeled using monocular images of head movement alone. As per our system's requirement, the human head motion trajectory in sagittal plane requires capturing human pose from front. Since the user would be standing in front of the camera on the treadmill, the chances of occlusion were eliminated.

Generally, motion captured through vision sensors is modeled based on object model [20], shape [21], or trajectory in 2D and 3D tracking space [22]. Hence several models based on a variety of techniques can be obtained for user-centered design of Human-Computer Interaction

applications. Among these motion models, the human head motion in sagittal plane was hypothesized to be similar to that of body center of mass. Various studies have been carried to obtain standardized motion models of human body center of mass in sagittal plane [23]. As an initial guess, it can be hypothesized that the head will follow somewhat same trajectory as body center of mass. However, these models could not be used in our system design as they are all developed by using contact sensors. Use of contact sensors gives accurate results, yet it can be a cause of hindrance in effective human computer interaction. Use of excessive hardware components also increases system's computational complexity compared to the off the shelf systems which can be customized and installed anywhere. Hence, the motion features were acquired using non-contact sensor only.

2.1. Motion Tracking

2.1.1. Tracker Selection

As part of preliminary research, a simple frame to frame detection strategy was adopted for basic hypothesis development. The algorithm used performed detection in each frame and then detected point was mapped from image to Cartesian plane. The algorithm was computationally inefficient taking time to first detect the features and then map them to Cartesian plane. It was also inaccurate as the face would be missed during quicker movements and there would not be enough points obtained for trajectory mapping.

Frame by frame detection becomes unnecessary in case of dynamic footage as information from preceding frames is not used for detection. Tracking on the other hand is an efficient and suggested approach for detecting object in dynamic footage due to its robustness and adaptation

to changes in viewpoints [24]. Tracker selection can be done based on features to be detected and tracking speed required. A comprehensive literature review was performed for tracker selection considering the two basic criteria for this study: robust tracking and higher processing speed. Currently, a variety of trackers exist, among which correlation filter-based trackers are highly preferred for real time tracking applications [25]. They are also reported to perform better in conditions like varying illumination, background clutters, occlusion, and changing camera postures. Correlation based trackers also show higher performance in tracking objects in high speed scenarios where missing the target due to motion blur is still a challenge due to high relative speed between target and camera [26].

In case of a person running on a treadmill with his face moving at higher velocity, we selected KCF tracker [27]. The tracker has been recognized by various studies for its higher processing speed, computational efficiency and low storage requirements [26, 29, 30]. However, using tracker alone with manual object and landmark detection could again result in inaccurate results in case of wrong initial guess. To avoid any detection or tracking error, a hybrid approach of detection and tracking was finally used. In our case the object to be detected is human face. Instead of manual object modeling and landmark identification, Haar-Cascade classifier proposed by Viola and Jones [28] was used to provide the tracker with accurately calculated initial tracking point. The classifier draws the bounding region of interest around the face of the running user on which the center of the region is selected as the landmark for tracker.

Once detected, the tracker tracks the face of the user and tracked trajectory is mapped from image to world plane. The features selected for tracking are raw pixels – the center pixels of the ROI as KCF shows satisfactory performance on raw pixels. HOG features can also be used for

better processing and tracking and can be used for future work. For this study, the results obtained with raw pixels were adequate for further processing and HOG features were avoided to keep maximum computational simplicity in the algorithm.

To ensure that the tracker meets our set criteria, KCF tracker was tested for its accuracy and robustness based on three standard criteria: center location error, area overlap, and success rate. The error analysis was performed based on tracking time as matching the time of the two trajectories would be the requirement of our control law. The precision plots were analyzed for average error for a dataset of 30 video sequences. Table 1 lists tracker's evaluation parameters for two videos giving standard and generalized trajectory and velocity mapping.

Average Center Location Error (CLE) is computed in pixels as:

$$CLE = \frac{1}{n}\sum_{i=1}^{n}\sqrt{\left(x_i^t - x_i^g\right)^2 + \left(y_i^t - y_i^g\right)^2} \tag{2.1}$$

Where $[x_i^t, y_i^t]$ denotes the tracked center pixel location of the object by the tracker and $[x_i^g, y_i^g]$ is the center pixel location of the ground truth. The error is computed over n number of frames. Here it is assumed that the center location of the detector acts as ground truth as it is obtained via efficient face detection and classification algorithm.

Area Overlap Ratio (AOR) is calculated from the interaction of bounding box drawn after detection and bounding box of the tracker such that:

$$AOR = \frac{area\ (G \cap T)}{area\ (G \cup T)} \tag{2.2}$$

Where G represents the area of the bounding box drawn through face detection algorithm acting as ground truth and T is the area of bounding box drawn by the tracker.

The average overlap area ratio is used to set the third evaluation criteria of Success Rate (SR). For a threshold of 50%, the correctly overlapped areas with a ratio higher than 0.5 indicate success. For a total *n* number of frames, the success rate is then calculated as:

$$SR = \frac{\sum_{i=1}^{n} Success}{n} \quad , \; success = \begin{cases} 1 & for\ AOR > 0.5 \\ 0 & for\ AOR < 0.5 \end{cases} \qquad (2.3)$$

Table 1 The evaluated (a) center location error (b) area overlap ratio and (c) success rate of KCF tracker for different fps

Video Dataset	**Motion**	**Features**	**Fps**	**CLE (pixels)**	**AOR**	**SR (%)**
1	Running	Raw Pixels	30	31.07	0.58	85%
2	Running	Raw Pixels	60	42.69	0.57	85%

The evaluation of tracker performance shows anomalies than its recorded performance accuracy in case of center location error threshold. The reasons noted for this deviation were assumed fixed distance of user from camera and imprecise preprocessing due to varying illumination conditions. Further, the anomalies can be catered in controller design.

2.1.2. Detection and Tracking

Figure 2 illustrates the algorithm designed for trajectory tracking and mapping. In the first frame, the algorithm detects face and computes a region of interest (ROI) around the face. Once the face is detected, the KCF tracker is initialized with the ROI computed by the face detector. KCF tracks the ROI in each frame by computing its Gaussian Kernel on grey pixels. For trajectory mapping, the center of the ROI is computed to calculate the head displacement in each frame. If the face is not detected in the first frame, the algorithm moves to the next frame until the face is detected. Similarly, if the KCF loses track due to occlusion or motion blur the KCF gives control back to the face detector algorithm.

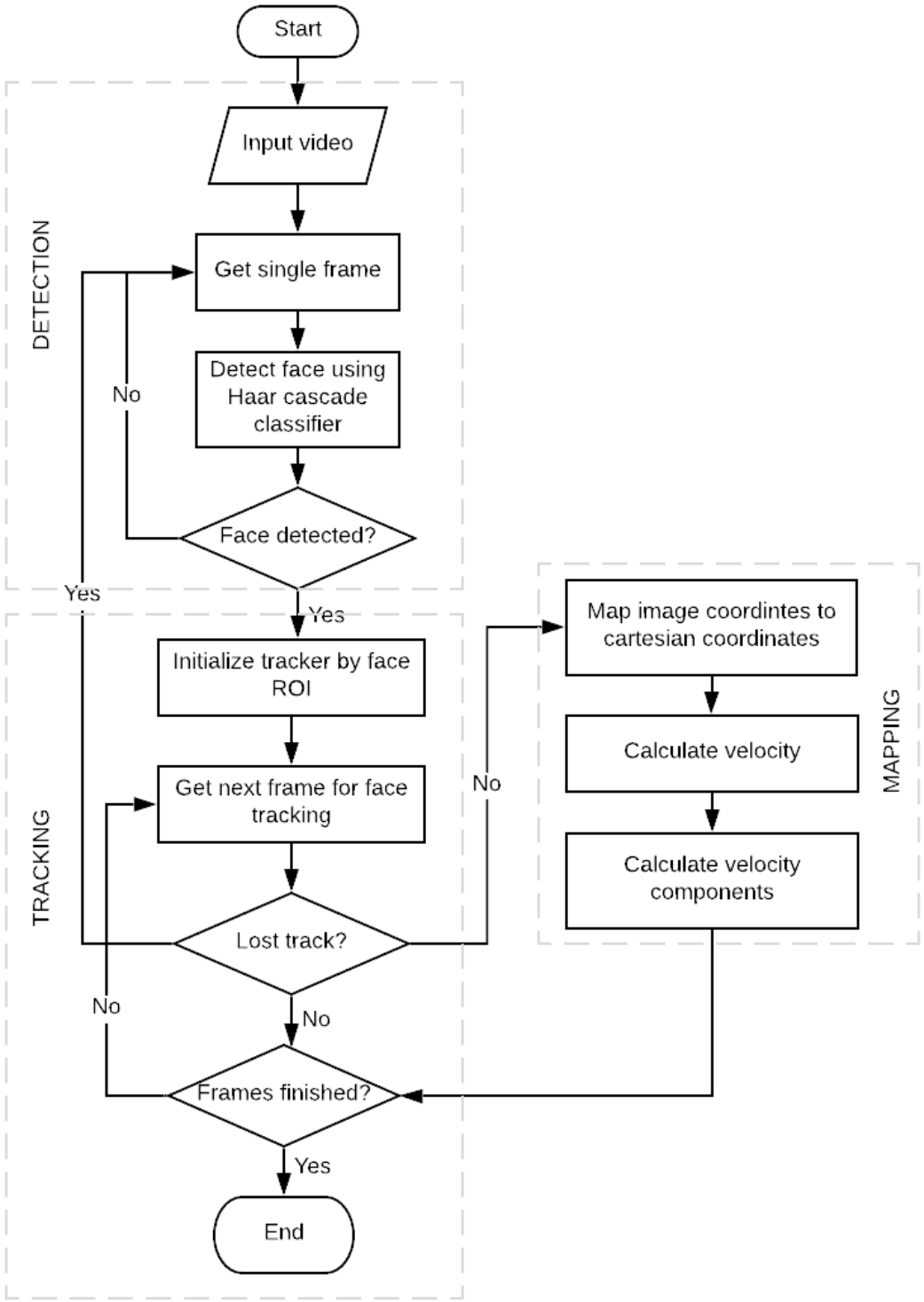

Figure 2: Head motion tracking and trajectory mapping algorithm

2.2. Trajectory Mapping

The trajectory is modeled by mapping the motion pixels based on the position of bounding box center in particular camera frames. Tracker is initialized by the bounding box obtained drawn around the face detected by Haar-Face Detector. The bounding box is then tracked frame by frame for a defined processing time which is the frames per second (*fps*) processing time of tracker in our case. After detection, the dimensions of bounding box drawn around user's face are obtained as:

$$b = [b_x \;\; b_y \;\; w \;\; h]$$

Here ($b_x \;\; b_y$) are the coordinates of the bounding box's origin and ($w \; h$) are the width and height of bounding box determined by the face detecting algorithm. To have a single trajectory mapping point (F_x, F_y), center pixel coordinates of the bounding box are computed using (2.4) and (2.5) as:

$$F_x = b_x + \frac{w}{2} \tag{2.4}$$

$$F_y = b_y + \frac{h}{2} \tag{2.5}$$

Each tracked point (F_x, F_y) is analyzed in Cartesian coordinate frame (x,y) for its velocity v at time t and direction α calculated using (2.6) till (2.9). While image pixel coordinates are mapped into Cartesian coordinates (in meters) using standard perspective projection as:

$$x = \frac{F_x}{f} \times z_{cam} \tag{2.6}$$

$$y = \frac{F_y}{f} \times z_{cam} \tag{2.7}$$

$$v_t = \frac{\sqrt{(x_i - x_{i-1})^2 - (y_i - y_{i-1})^2}}{fps} \tag{2.8}$$

$$\alpha_t = \tan^{-1} \frac{(y_i - y_{i-1})}{(x_i - x_{i-1})} \tag{2.9}$$

Subscripts *i* and *i-1* represent successive frames being tracked. For these calculations, we assume the distance from the camera $z_{cam}$to be constant as it changes negligibly while running on a treadmill and was not found to affect the results. Equation (2.10) is used to calculate the horizontal and vertical components of the velocity at any time *t.*

$$v_t^x = v_t \cos \alpha \tag{2.10}$$

$$v_t^y = v_t \sin \alpha \tag{2.11}$$

2.3. Trajectory Analysis

Twenty subjects were selected for experiment and trajectory analysis purpose. Tracking was performed for 'fixed camera-moving object' motion setup. Every person's face was tracked for two motion taxonomies: Walking and Running. The videos were captured at two frame rates of 30fps and 60 fps with a resolution of 1280x720. Figure 3 shows the experimental setup for data acquisition for user running at a treadmill at higher speed.

In order to evaluate the algorithm a video database of 30 subjects is recorded, which includes 22 males and 8 females with no known gait abnormalities. We used Agrocam Pro RGB digital camera [29] with CMOS BSI image sensor for video recording.

Experiments are performed on treadmill for walking speed of *4mph (1.78 m/s)* and *6mph (2.68 m/s)* and a racing speed of 8mphh *(3.57 m/s)* and *10mph (4.47 m/s)*. Among 30 subjects, 16 were familiar with running or walking on a treadmill and had no difficulty running or walking on it, while 14 subjects were using the treadmill for the first time. Figure. 3 shows experimental setup and camera mount for recording videos.

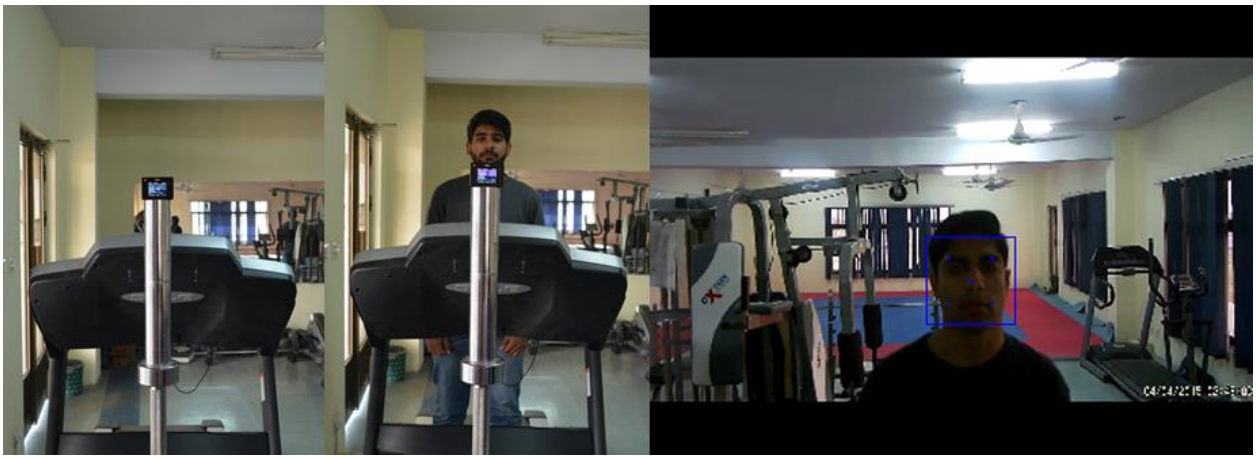

Figure 3: Experimental setup to capture head motion trajectory

The run-time performance of the algorithm was tested on a 3.40 GHz Intel® Core i7-6700 processor with 64-bit Ubuntu 16.04 LTS operating system. Videos were recorded at 60 fps with a resolution of 720x1080. The camera was calibrated to find the camera intrinsic parameters using MatLab® Camera Calibration Toolbox. A graphical user interface was developed in Qt framework for the analysis of video sequences as illustrated in Figure 4. Table 2. summarizes the experimental dataset.

Table 2 Experimental Dataset

No. of subjects	30	No. of video sequences	60
Age group	20-25 yrs	Frames per second	30,60

Female subjects	8	Male subjects	22

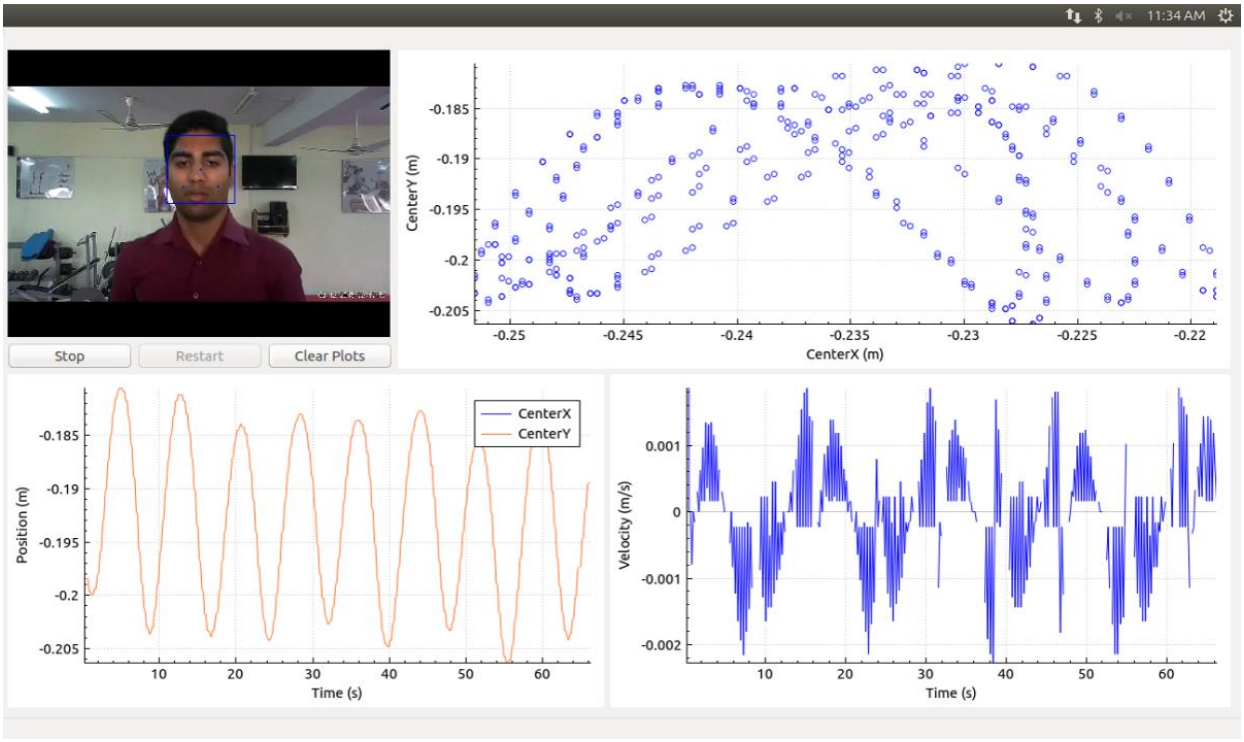

Figure 4: GUI developed for offline trajectory analysis

For each sequence, the head motion displacement and velocity components were computed and plotted. The head motion trajectories were analyzed to distinguish between walking and running sequence for the users who had no difficulty using the treadmill. Figure 5 and Figure 6 show the general walking and running trajectories mapped in sagittal plane at different velocities. It is shown that the head of the user traces a convoluted loop during walking and running locomotion. Individual strides shown were obtained based on single cycle calculated by extracting the respective horizontal and vertical maxima from the walking and running sequences. The results are further validated for the fact that, when mapped in sagittal plane, the loop circulates anticlockwise for walking and clockwise for running. The results obtained were similar to those

obtained by studies conducted to analyze body center of mass trajectories. Trajectories do not differ in case of male or female users but do fluctuate in case of other movements while moving such as turning face away from camera and occluding face with hands

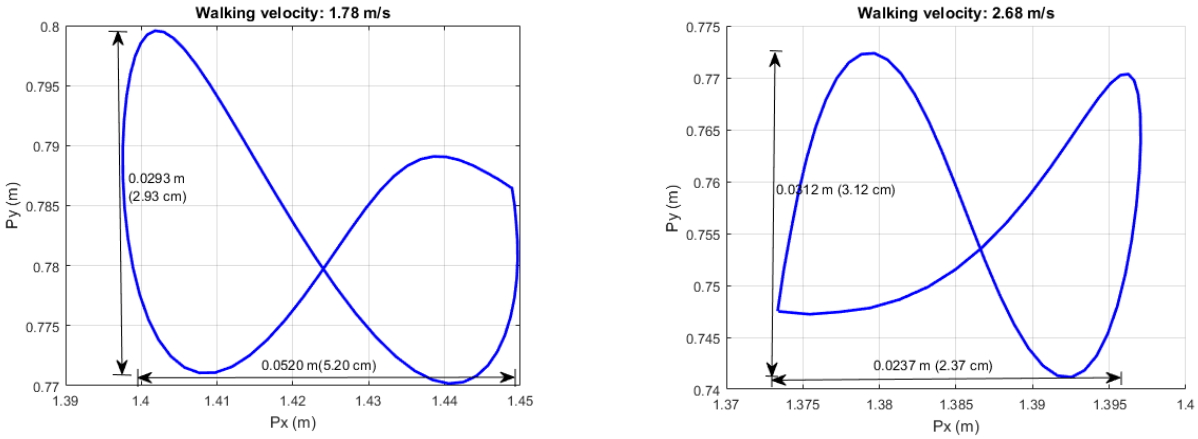

Figure 5: Head motion trajectory mapped in sagittal plane at two walking velocities: 1.78 m/s and 2.68 m/s

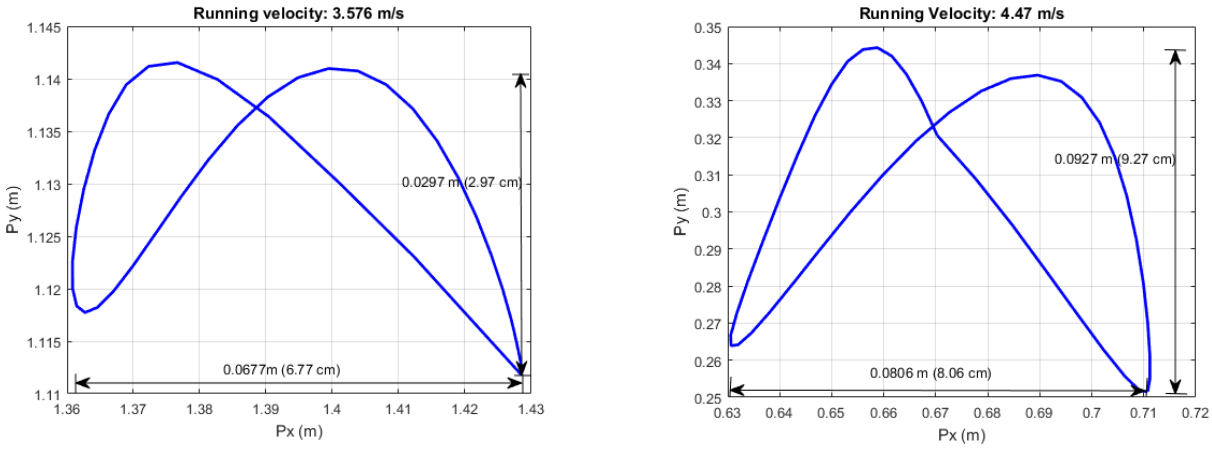

Figure 6: Head motion trajectory mapped in sagittal plane at two running velocities: 3.57 m/s and 4.47 m/s

Figure 7 and Figure 8 show the lateral (in x-axis) and vertical (in y-axis) head movement pattern during walking and running respectively over a period of time. In each figure, First column shows change in position while second column shows the respective change in velocities in lateral and vertical direction. During each walking and running sequence, one cycle of lateral motion is accompanied by two cycles of vertical motion. The two peaks in vertical axis correspond to the change in head's position with motion of left and right foot. The velocity also follows a periodic trend but it keeps varying even in a single cycle. The blue arrows point out the abnormal peaks in velocity during walking which shows walking in general comprises of inconsistent velocities while running velocity is more consistent and periodic.

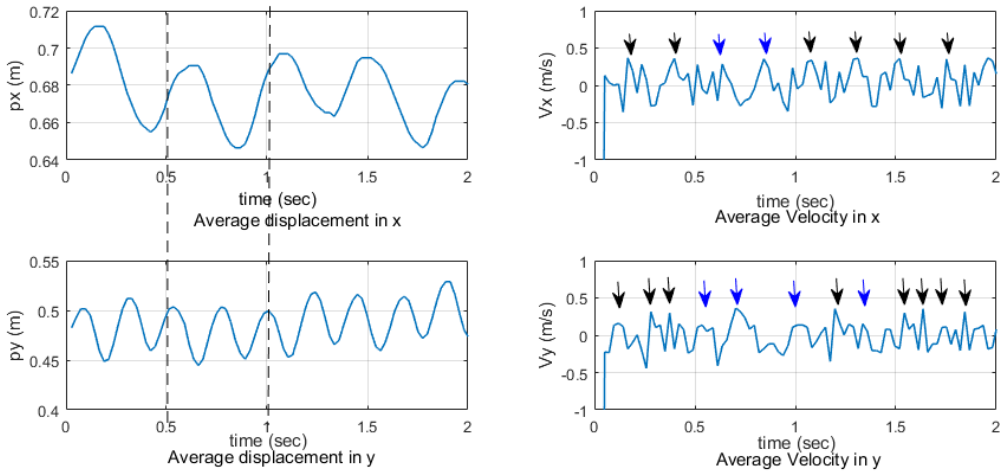

Figure 7: Comparison of head displacement and velocity in 2D sagittal plane while walking at speed of 2.68 m/s

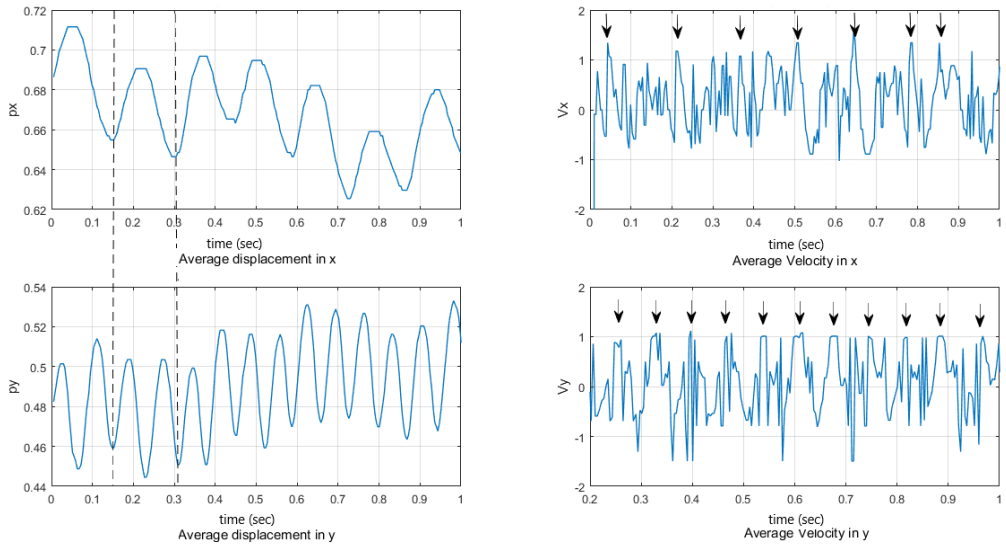

Figure 8: Comparison of head displacement and velocity in 2D sagittal plane while running at speed of 4.47 m/s

Table 3. lists the average displacement and velocity of the head computed. The calculated results show that the walking and running sequences can be differentiated based on the values of displacement and velocity obtained. The results are quantified for different locomotion patterns that can be identified with corresponding head velocities.

Table 3 Average head velocities for walking and running at selected speeds

Sequences **Treadmill velocity**	**$Disp_x$** **m**	**$Disp_y$** **m**	**Avg v_x** **m/s**	**Avg v_y** **m/s**	**Avg v_{total}** **m/s**
Walk (*1.78 m/s)*	0.044	0.029	0.0035	0.0041	0.0044
Walk (*2.68 m/s*)	0.029	0.040	0.0039	0.0051	0.0057
Run (*3.57 m/s*)	0.070	0.089	0.083	0.0084	0.0084
Run (*4.47 m/s*)	0.067	0.043	1.1061	1.2393	1.4280

Both graphical and numerical data shows that head movements in both lateral and vertical axis are significantly clear in running as compared to walking. The increase in stride length

correspond to increased head displacement. This affects the vestibular coordination of visual input and posture balance negatively and results in increased sway. This reasons for the asymmetry in the trajectory which is less significant in walking and more in running patterns. Similar results have been reported by studies performed to analyze the relationship of treadmill walking and running with gaze and balance [30]. The studies validate the fact that balance in sagittal plane is not disturbed due to treadmill rather lack of optical cues for vestibular calibration causes conflicting visual information and results in impaired postural stability even for a healthy individual.

CHAPTER 3: SYSTEM DESIGN

3.1. Mathematical Modeling

The generalized trajectory of obtained resembles a figure 8 trajectory which is a form of Lissajous trajectory [31]. Lissajous trajectory finds its application in various biomechanical [32], mechanical [33], and electrical [34] problems. The common parallel manipulator configurations used for mechanical linkages tracing Lissajious trajectory are four bar and five bar mechanisms. The design of a mechanism for present case requires two conditions:

1. The linkage should trace a symmetric figure 8 trajectory
2. The point tracing the trajectory should be located at the linkage that remains fixed in horizontal plane

These two conditions ensure the vibration free synchronized motion of the screen or any object that will be placed on the mechanical linkage. Evidence suggested by various studies supports that a figure 8 trajectory of desired symmetry can be obtained by controlling the motion parameters and link length/arrangements for four and five bar linkages [35] [36]. Yet these designs have a significant drawback of rotating the end effector along with linkages. Hence, there was a requirement for a novel design that would keep the end effector in the same plane as that of user's trajectory. The platform proposed by Lin and Koichi [16] has the feature of keeping the end effector in plane. The specifications of the parallel manipulator are further explained in geometrical analysis.

Mechanism design and vector loop equation for the mechanical model is shown in Figure 8, which is further divided in two vector loops as shown in Figure 9. Provided the new 8 bar linkage design for target tracking, the kinematics analysis has been performed using absolute forward kinematics and vector loop equations.

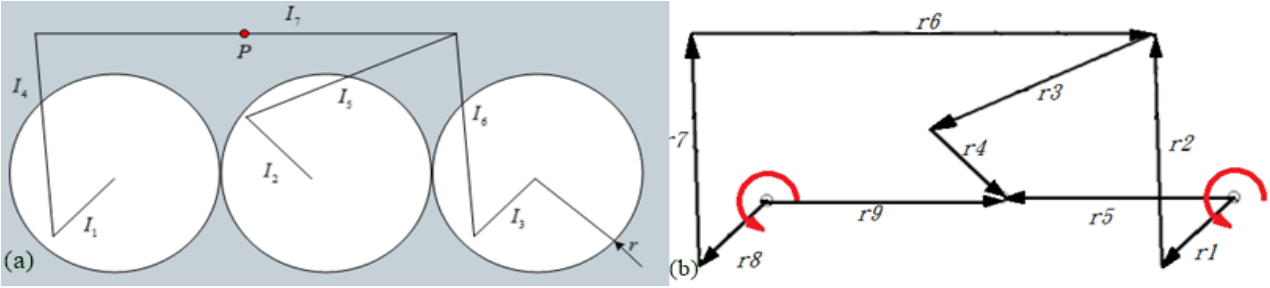

Figure 9: (a) mechanical design of the geared eight bar mechanism (b) vector loop diagram of the system

As shown in the figure the seven links in the mechanism are named as $\boldsymbol{I_1}$ through $\boldsymbol{I_7}$ and when we draw the vector diagram the total vectors become nine (adding additional vectors for links formed by two gears) respective lengths represented by radii are named as $\boldsymbol{r_1}$ through $\boldsymbol{r_9}$ respectively. The *"r"* is the pitch circle radius of the gear used to construct mechanism. The point *"P"* is the point of interest in the mechanism, it the point on which the display device supposed to be mounted and all calculations are done by keeping this point central it is also the center point of link $\boldsymbol{I_7}$.

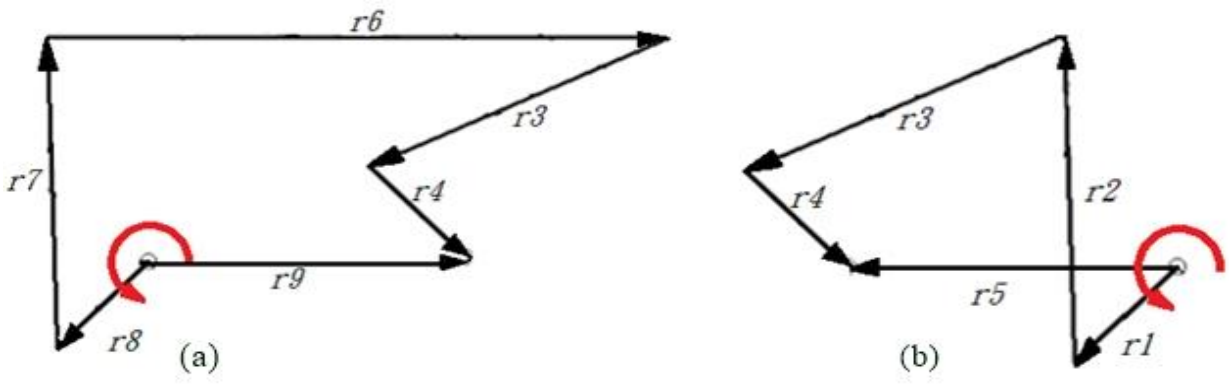

Figure 10: Two vector loops for mathematical modeling

Considering first loop (Figure 2-b), for an input of θ_1,

$$r_1 cos\theta_1 + r_2 cos\theta_2 + r_3 cos\theta_3 + r_4 cos\theta_4 = r_5 \cos\theta_5 \quad (3.1)$$

$$r_1 sin\theta_1 + r_2 sin\theta_2 + r_3 sin\theta_3 + r_4 sin\theta_4 = r_5 \sin\theta_5 \quad (3.2)$$

Rearranging to separate the unknowns θ_2 and θ_3

$$r_2 cos\theta_2 + r_3 cos\theta_3 = r_5 \cos\theta_5 - r_4 cos\theta_4 - r_1 cos\theta_1 \quad (3.3)$$

$$r_2 sin\theta_2 + r_3 sin\theta_3 = r_5 \sin\theta_5 - r_4 sin\theta_4 - r_1 sin\theta_1 \quad (3.4)$$

From geometry,

$$\theta_8 = \theta_1, \theta_5 = \theta_9 = 180^o, \text{ and } \theta_4 = 180^o - \theta_1 \quad (3.5)$$

Equations (3.3) and (3.4) are solved simultaneously using Newton Raphson method to find θ_2, θ_3 and $\frac{d\theta_2}{d\theta_1}$, $\frac{d\theta_3}{d\theta_1}$.

Similarly, for output loop (Figure 10-a),

$$r_3 \cos\theta_3 + r_4 \cos\theta_4 + r_6 \cos\theta_6 + r_7 \cos\theta_7 + r_8 \cos\theta_8 = r_9 \cos\theta_9 \qquad (3.6)$$

$$r_3 \sin\theta_3 + r_4 \sin\theta_4 + r_6 \sin\theta_6 + r_7 \sin\theta_7 + r_8 \sin\theta_8 = r_9 \sin\theta_9 \qquad (3.7)$$

θ_6, θ_7 and $\frac{d\theta_6}{d\theta_1}$, $\frac{d\theta_7}{d\theta_1}$ can be calculated following the same procedure using eq (3.5) and (3.7) while $\frac{d\theta_8}{d\theta_1} = 1$.

For the position vector OP in Figure 10, the linear displacement and linear velocity of the point P can be found using equation (3.8 – 3.11)

$$r_{px} = 0.5 \times r_6 \cos\theta_6 + r_7 \cos\theta_7 + r_8 \cos\theta_8 \qquad (3.8)$$

$$r_{py} = 0.5 \times r_6 \sin\theta_6 + r_7 \sin\theta_7 + r_8 \sin\theta_8 \qquad (3.9)$$

$$v_{px} = -0.5 \times r_6 \sin\theta_6 \frac{d\theta_6}{d\theta_1} \times \frac{d\theta_1}{dt} - r_7 \sin\theta_7 \frac{d\theta_7}{d\theta_1} \times \frac{d\theta_1}{dt} - r_8 \sin\theta_8 \frac{d\theta_8}{d\theta_1} \times \frac{d\theta_1}{dt} \qquad (3.10)$$

$$v_{py} = 0.5 \times r_6 \cos\theta_6 \frac{d\theta_6}{d\theta_1} \times \frac{d\theta_1}{dt} + r_7 \cos\theta_7 \frac{d\theta_7}{d\theta_1} \times \frac{d\theta_1}{dt} + r_8 \cos\theta_8 \frac{d\theta_8}{d\theta_1} \times \frac{d\theta_1}{dt} \qquad (3.11)$$

While angular velocity of gear 1 corresponding to θ_1 can be computed by solving the equations (3.12) and (3.13)

$$v_p = \sqrt{v_{px}^2 + v_{py}^2} \qquad (3.12)$$

$$\omega_1 = \frac{d\theta_1}{dt} = \frac{v_p}{\sqrt{a^2+b^2}} \qquad (3.13).$$

where,

$$a = -0.5 \times r_6 \sin\theta_6 \frac{d\theta_6}{d\theta_1} - r_7 \sin\theta_7 \frac{d\theta_7}{d\theta_1} - r_8 \sin\theta_8 \frac{d\theta_8}{d\theta_1} \quad (3.14)$$

$$b = 0.5 \times r_6 \cos\theta_6 \frac{d\theta_6}{d\theta_1} + r_7 \cos\theta_7 \frac{d\theta_7}{d\theta_1} + r_8 \cos\theta_8 \frac{d\theta_8}{d\theta_1} \quad (3.15)$$

Figure 11 shows the results of interest obtained by solving equation numerically using MATLAB. The MATLAB results show a somewhat constant angular velocity obtained for a constant input velocity of 60rpm.

3.2. Model Analysis

The manipulator design has been evaluated for trajectory by two methods: solving mathematical model in MATLAB and analyzing geometry in SOLIDWORKS. In SOLIDWORKS, the mechanism was designed as per given specifications and analysis was performed to measure phase change in trajectory at various link lengths. Kinematic analysis performed in MATLAB show that given a constant input angular velocity to gear 1 result in a sagittal symmetric figure 8 trajectory traced by the point P. Results are also verified by simulating the mechanism design in SOLIDWORKS (Figure 11) and are in consistence with MATLAB results.

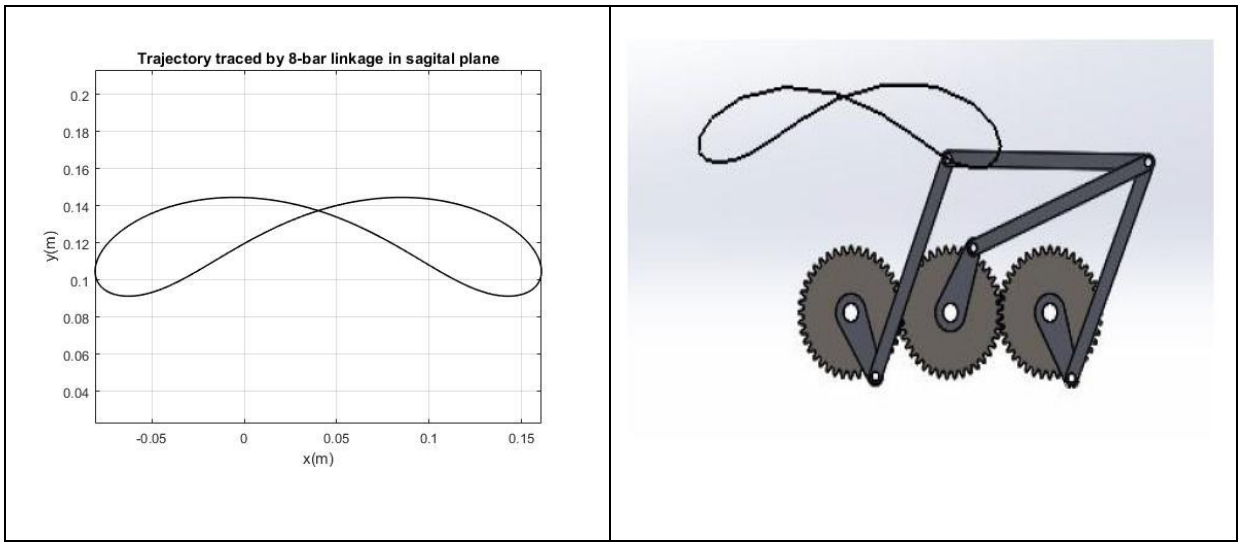

Figure 11: Comparison of manipulator trajectory through mathematical; modeling and geometry design

CHAPTER 4: CONTROLLER DESIGN

4.1 Vision Based Control:

The parallel robotic configurations are controlled via Inverse kinematic models instead of Forward Kinematics. This eliminates the need of iterative solutions and avoids the convergence issues as discussed previously. However, controlling parallel robots using system´s dynamics also has other problems. Among many other, concerning the motion control a significant problem is of system´s redundancy. While forward kinematics helps defining a unique pose of the end effector of a serial robot for a set of unique joint variables; the end effector pose for a parallel robot can be achieved by various link configurations which again leads to numerical instabilities. These problems are solved while controlling a parallel robot through visual servoing.

Controlling a mechanical component, commonly robot, using visual feedback from the environment is usually termed as *visual servoing*. The visual servoing is independent of joint sensing [37] and is performed utilizing visual features to define control variables. These visual features include points, lines, and regions of interest in an image. The approaches used for visual servoing control are position-based and Image/feature-based. In position based visual servoing, the visual data is used to construct the 3D pose of the robot. The kinematic error and actuator commands are all mapped to Cartesian space. The control scheme developed for this study relies on the principles of position based visual servoing. In image based visual servoing all the error and pose calculations are performed in image plane.

There exists various control algorithms based on position-based visual servoing for both series and parallel manipulators. A common approach incorporating position-based visual servoing for both serial and parallel robots is using predictive control law in which the position of the moving object is predicted for the next time frame using the acceleration information of current frame and error of the position achieved in previous consecutive points [38] [39]. The simpler form of robot control is through PD control based on position based visual servoing. This control approach is most widely used for controlling parallel manipulators [40] [41]. This study illustrates the control of the 8 bar parallel robot using position based PD control.

4.2 Parallel Manipulator Control Algorithm

The user and platform interfacing aim to achieve platform's motion that is in sync with user's head motion. This requires two parameters: the platform should move with same frequency and be in same phase as that of user's head. For this synced motion, the controller would require two inputs:

1. Visual input from camera to assess user's motion parameters
2. Angular input from mechanism to assess its angular motion parameters.

As a result, the speed of motor rotating the mechanism is controlled to achieve desired platform motion. The overall hardware software interfacing is illustrated in Figure 12 below.

The interfacing involves implementation of two modules in parallel: face detection and tracking of user and synchronization of moving platform with user's head trajectory (Table 4 and Table 5). For detection and tracking, the process is initiated with capturing user's image from the USB

camera. The camera sends real time video feed to Raspberry Pi, which processes each frame to iteratively detect a human face closest to camera. The detection algorithm starts by capturing first frame of the video and detecting user's face in it using Haar-Cascade Classifier. Once the user's face is detected, the bounding box containing relevant pixels is passed to a Kernelized Correlation Filters (KCF) Tracker, which then tracks the pixels pertaining to face of user in subsequent frames. This results in successful tracking of user's face throughout motion. The coordinates of bounding box center are used to map traced trajectory, displacement, and velocity in meters in real-time on the associated GUI.

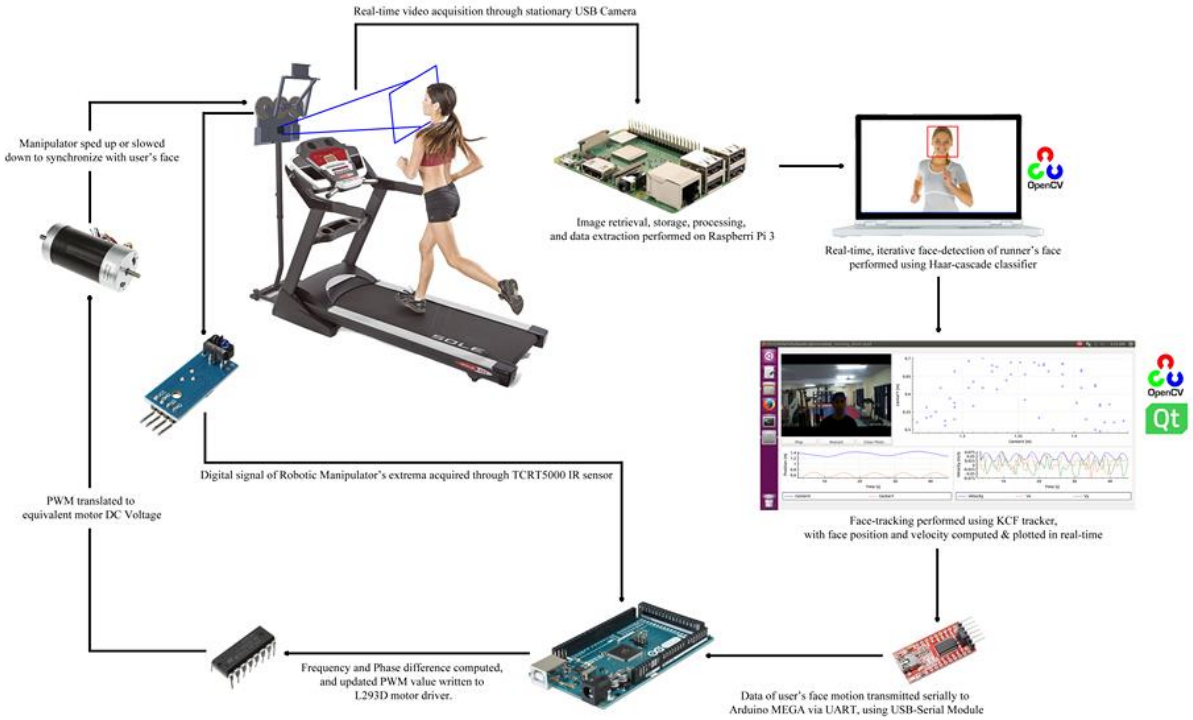

Figure 12: User-Platform interface design based on real-time video feedback obtained from stationary camera

For motion synchronization, every time the face of user hits a specific x-extremum of formed trajectory, a signal is sent through UART serial protocol to the Arduino microcontroller which then controls motor speed of robotic manipulator. To determine if the end effector is at required x-extremum, a marker is placed on the rotating gear, which is read off by an IR sensor. This is possible because one complete rotation of the gear pertains to one complete cycle of user's face trajectory.

Table 4: Pseudo code for face detection and tracking to get maxima of user trajectory

Input: *Video frames*

Output: *x-maxima of user trajectory*

for input video frames available **do**
  if tracker not initialized **or** tracker has failed
    1. Run Haar Cascade Classifier on frame to detect face
    2. **if** face detected
        1. Get ROI
        2. Initialize KCF Tracker with frame and ROI
      else
        1. Skip rest of code and get next frame
      end if
  end if
    3. Update tracker with frame and get latest ROI
    4. Compute (x, y) of centroid of ROI in meters
    5. Check values of x in decreasing order
    6. **if** x value is greater than previous x value
       Send x value through serial signal to controller
      end if
end for

Table 5: Pseudo code for synchronization of moving platform with user's head trajectory

Input: *x-maxima of user trajectory, x-maxima of hardware trajectory*

Output: $Frequency\ ratio \rightarrow 1$ and $Time\ difference \rightarrow 0$

while 1
    if mechanism just started
        1. Set motor PWM
        2. Stop motor at x-maxima of hardware trajectory
        3. while x-maxima of user trajectory not received

```
            a. wait
            b. calculate time period of user trajectory
    end if
    if x-maxima of hardware trajectory is detected
        1. increment hardware maxima count and calculate time period of hardware trajectory
    end if
    if x-maxima of user trajectory is detected
        1. increment user maxima count calculate time period of user trajectory
    end if
    if user maxima count == hardware maxima count
        1. perform frequency matching by multiplying frequency ratio to PWM
    end if
    compute time difference for both trajectories to reach maxima
    if time difference ≫ 0
        1. decrease PWM to reach nearest extrema
        2. while x-maxima of user trajectory not received
            a. wait
        3. start with previously obtained frequency ratio
    end if
End while
```

As soon as the signal is received, the end-effector is started at a certain speed, and is made to trace an iteration of figure-8 trajectory, until it reaches its starting point. This time period for end-effector is recorded. The time period for a user's trajectory is determined by recording the delay between signals sent by Raspberry Pi. The error between time periods is minimized by multiplying manipulator motor speed with this 'frequency' ratio, known as Frequency Matching in our control. Frequency matching ensures speed control, but does not ensure position control, which is achieved through Phase Matching. In Phase Matching, the difference between time periods is calculated, and is checked to be within a specific threshold. If this difference exceeds the threshold, the end effector is made to wait at the starting x-extremum as in beginning, and is resynchronized with the face of user when user reaches the same extremum. The thresholds for phase matching are specified for various motor speeds, determined through trial-and-error methods.

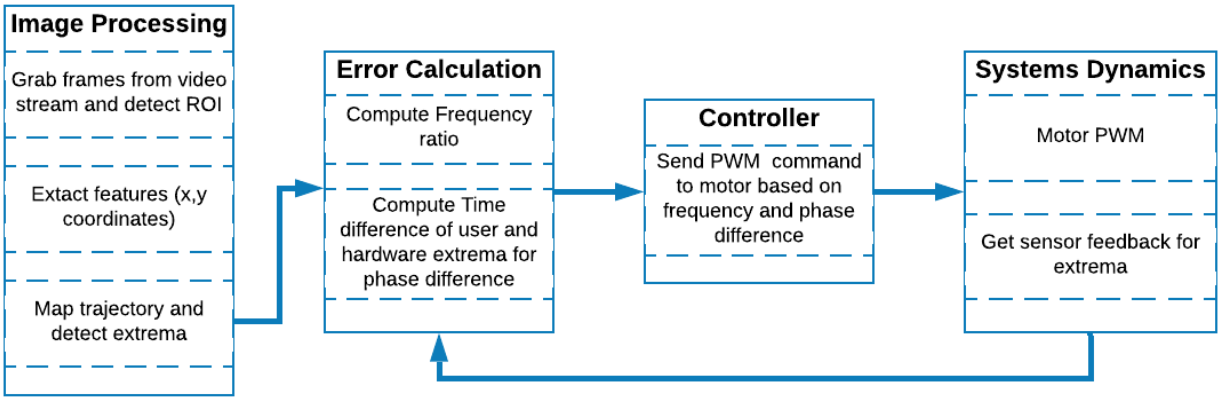

Figure 13: Platform synchronization control

CHAPTER 5: IMPLEMENTATION AND RESULTS

To evaluate the usability of platform, the same 30 users who performed test runs for obtaining generalized trajectory performed test run with the system mounted in front of treadmill. The rotating platform was placed on a stationary support at an optimum distance from the treadmill from where the users could read the text displayed on the screen. The users were asked to run on four set speeds on treadmill: walking speed of *4mph (1.78 m/s)* and *6mph (2.68 m/s)* and a racing speed of *8mphh (3.57 m/s)* and *10mph (4.47 m/s)*.

Figure 14: Experimental Setup: the platform is placed stationary in front of the user at a fixed distance from the treadmill

Following the training exercise, the individuals were asked to complete post study interview to record their feedback on interaction with the platform. The platform functioning was also observed during the test runs and observations were recorded for further analysis on design optimization.

Two cases were set for performance analysis of the system: a single user running at changing speeds, and multiple users running at fixed speed. The results for both cases are listed in Table 6. Results obtained illustrate that the platform showed satisfactory results at jogging and slow running speeds.

Table 6 Success rate of prototype testing for users running at selected treadmill speeds

Treadmill Speeds	No. of Trials	No. of Successful Tracking	No. of false positive	Success rate
1.78 m/s	30	25	5	83.33%
2.68 m/s	30	28	2	93.33%
3.57 m/s	30	26	4	86.67%

Test runs were also performed for faster running speed of 4.47 m/s and success rate of 46.66% was obtained. For higher running speed of it was challenging for the users to focus on the platform. The reason can be a lag in platform tracking due to unavailability of clear visual cues. This can be because of time delay between the phase shift of the user's head trajectory and platform. As shown in the kinematic analysis of head motion, the displacement and velocity pattern of head motion are significantly prolonged than walking patterns. This implies the head shaking movement is also quite significant for running. This contributes more to postural sway and subsequently results in larger error.

As faster speeds are not usually recommended for rehabilitation trainings, this was considered a minor anomaly in system. Users' training on the platform was also a factor as reading from screen was more challenging for users who needed training on the treadmill. On the other hand, previously trained subjects were rather comfortable with reading while walking and running. For selected speeds, there were no errors recorded in synchronization of platform's movement with

user's head movement. The test users overall showed satisfaction on the use of platform. It was interactive and fun activity to read something while walking or running. To further endorse practice results, Comparison of frequency ratio obtained for the three selected speeds was also performed as shown in Figure 8. An analysis of mean frequency ratio and standard deviation of the data obtained (Table 7) shows successful synchronization of the platform with users' head motion.

Table 7 Average frequency ratio obtained for motion synchronization at three selected speeds

Selected Speeds	No. of Trials	Mean Frequency Ratio	Standard Deviation
1.78 m/s	30	1	0.0269
2.68 m/s	30	1.005	0.0526
3.57 m/s	30	0.99	0.1046

The results were also plotted for comparison and analysis. The frequency plots shown in Figure 15 show that the two trajectories had an approximate frequency ratio of 1 when the user's speed is slow. There are more anomalies at higher running speeds. The anomalies are again caused by the two contributing factors: user's asymmetric trajectory and the distance from the camera that keeps changing due to lack of coordination among vestibular organs while locomoting in sagittal plane. Figure 15 shows the randomness of results obtained. Due to various environmental, biological, and data processing errors, the system keeps a continuous search of achieving a frequency ratio of 1. Based on these observations, we suggest further refining of control algorithm and geometrical parameters for better synchronization.

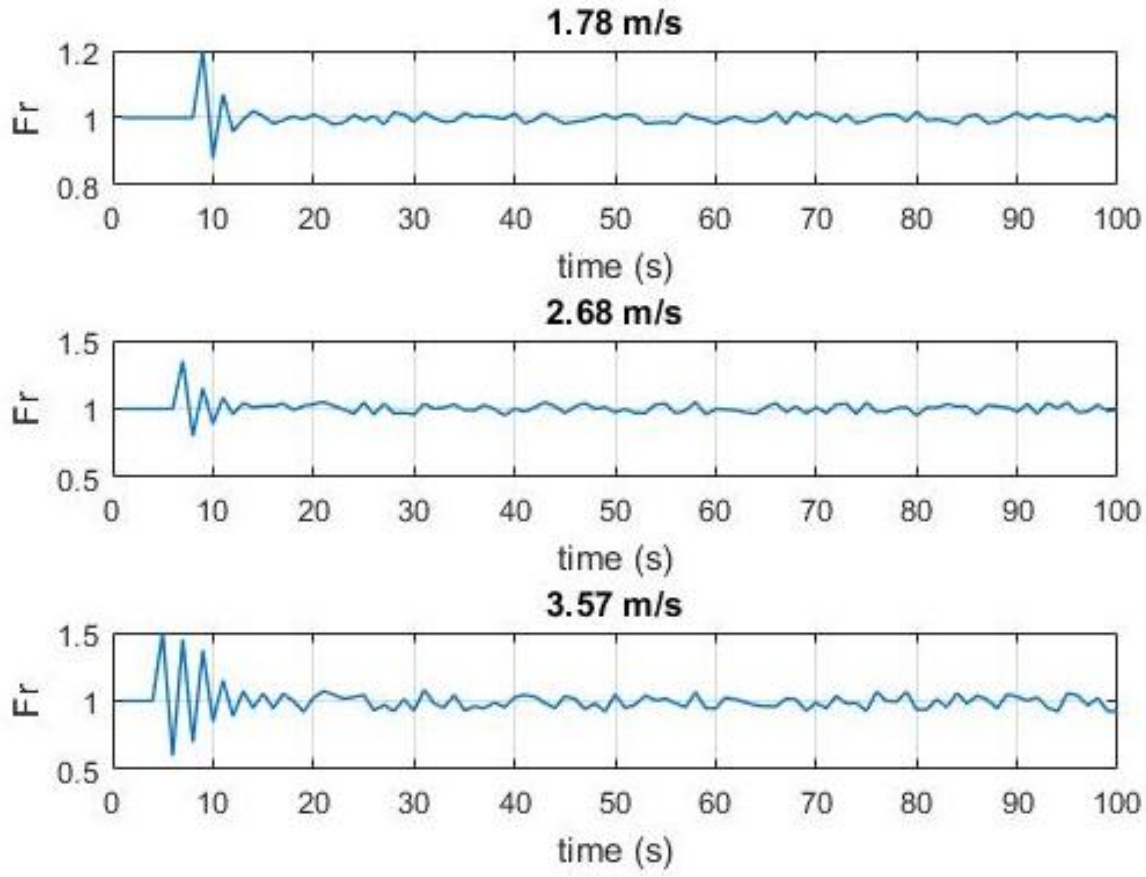

Figure 15: Comparison of frequency ratios at selected speeds

CHAPTER 6: CONCLUSION AND FUTURE WORK

The research proposes the design of a user centered motion tracking platform that can imitate the head motion of a running individual. The purpose is to minimize the relative velocity between running individual's head and the platform so that any screen placed on it seems stationary. The presented system is a proof of concept for the further development of a robust treadmill platform controlled by human head motion through visual servoing. Results obtained with an average success rate of 87.77% show the developed system's reliability for future development. The system has a high scope of importance in biomedical and related vestibular rehabilitation and sports applications. For higher running speed of it was challenging for the users to focus on the platform. The reason can be a lag in platform tracking due to unavailability of clear visual cues. This can be because of time delay between the phase shift of the user's head trajectory and platform.

Future research plans on improving the motion synchronization strategy for the platform based on robust machine vision and robotic interfacing control algorithms. Currently, the prototype is designed for fixed link length which was a hindrance in smooth synchronization of the platform with user's head motion. Future design includes adjustable link lengths so that maximum optimum trajectory of platform similar to user's trajectory can be obtained. Further, the current design does not incorporate the height adjustment mechanism and is planned to be incorporated in future designs. The design will allow platform adjustment on a stationary stand according to required height of the treadmill and the user.

REFERENCES

[1] C. T.-D. P. P. M. S. E. a. C. M. González-González, "Including gamification techniques in the design of TANGO: H platform," 2013.

[2] N. V. B. H. C. L. M. H. J. a. V. d. L. H. Shirzad, "FEATHERS, a bimanual upper limb rehabilitation platform: a case study of user-centred approach in rehabilitation device design".

[3] R. J. S. D. M. K. H. a. J. O. B. Reed-Jones, "Vision and agility training in community dwelling older adults: Incorporating visual training into programs for fall prevention".

[4] K. M. R. a. J. H. Szturm Tony, "Home-based computer gaming in vestibular rehabilitation of gaze and balance impairment," *Games for health journal, 4(3),* , pp. 211-220, 2015.

[5] W.-L. H. S.-H. W. C.-L. K. Po-Yin Chen, "Interactive wiimote gaze stabilization exercise training system for patients with vestibular hypofunction".

[6] I. O. L. v. K. P. U. D. K. P. a. J. M. H. Lansink, "Effects of interventions on normalizing step width during self-paced dual-belt treadmill walking with virtual reality, a randomised controlled trial".

[7] a. M. H. Stanley Jennifer, "A novel video-based paradigm to study the mechanisms underlying age-and falls risk-related differences in gaze behaviour during walking".

[8] V. A. P. A. C. a. U. D. C. Serchi, "Tracking gaze while walking on a treadmill: spatial accuracy and limits of use of a stationary remote eye-tracker".

[9] S. F. R. P. t. C.-Y. C. A. “. R. Belinda Lange, "Development of an Interactive Game-Based Rehabilitation Tool for Dynamic Balance Training," 2010.

[10] B. C. C. S. E. N. B. R. A. a. B. M. Lange, "Development and evaluation of low cost game-based balance rehabilitation tool using the Microsoft Kinect sensor," in *2011 Annual International Conference of the IEEE Engineering in Medicine and Biology Society P. 1831-1834*, 2011.

[11] "Effective game use in neurorehabilitation: user-centered perspectives".

[12] B. A. A. P. Skidmore J, "Variable Stiffness Treadmill (VST): System Development, Characterization, and Preliminary Experiments," *IEEE/ASME Transactions on Mechatronics,* vol. 20, no. 4, pp. 1717-24, 2014.

[13] K. M. R. &. J. H. T. Szturm, "Home-based computer gaming in vestibular rehabilitation of gaze and balance impairment," *Games for health journal, vol. 4, pp. 211-220, Jun 2015.*

[14] T. M. P. M. J. S. B. S. S. a. S. V. Szturm, "The interacting effect of cognitive and motor task demands on performance of gait, balance and cognition in young adults 2013".

[15] B. C. D. R. B. K. S. B. S. O. E. C. F. a. H. A. R. Rider, "Psycho-physiological effects of television viewing during exercise".

[16] Chi Yeu Lin and Koichi H, "Device capable of adjusting images according to body motion of user and performing method thereof". United States Patent US 8,926,475, 6 Jan 2015 .

[17] H. K. Chyi-yeu Lin, "Device capable of adjusting images according to body motion of user and performing method thereof". United States Patent 8,926,475, 06 01 2015.

[18] C. a. H. K. Lin, "Performing method of device capable of adjusting images according to body motion of user". United States Patent 9,223,400, 29 12 2015.

[19] A. N. M. Y. T. M. Bellakehal S, "Vision/force control of parallel robots," *Mechanism and Machine Theory,* vol. 10, no. 46, pp. 1376-95, 2011.

[20] F. A. a. R. C. R. Vemulapalli, "Human action recognition by representing 3d skeletons as points in a lie group," in *Proc. IEEE Conf. computer vision and pattern recognition, 2014, pp. 588-595.*.

[21] L. B. H. B. a. C. Y. H. Hai, "Interaction System of Treadmill Games based on depth maps and CAM-Shift,"," in *IEEE 3rd International Conference on Communication Software and Networks, 2011, pp. 219-22.*

[22] M. D. e. al, "3D human action recognition by shape analysis of motion trajectories on riemannian manifold," *IEEE Trans. cybernetics., vol. 45, no. 7, pp. 1340-1352, Sep 2014.*

[23] R. V. C. C. P. L. Tesio L, "The 3D path of body centre of mass dur- ing adult human walking on force treadmill," *Journal of biomechanics. 2010 Mar 22;43(5):938-44.*

[24] Y. v. Wettum, *Facial Landmark Tracking on a Mobile Device,* University of Twente, 2017.

[25] H. Z. T. D. Chen Z, "An experimental survey on correlation filter-based tracking," *arXiv preprint arXiv:1509.05520. 2015 Sep 18.*

[26] L. H. H. B. C. Z. Xu L, "Real-time robust tracking for motion blur and fast motion via correlation filters," *Sensors. 2016 Sep;16(9):1443.*.

[27] C. R. M. P. B. J. Henriques JF, "High-speed tracking with kernelized corelation filters," in *IEEE Transactions on Pattern Analysis and Machine Intelligence' 37 (3), 583-96*, 2015 March 1 .

[28] a. M. J. P. Viola, "Rapid object detection using a boosted cascade of simple features," in *CVPR, vol. 1, pp. 511-518, Dec 2001*.

[29] A. C. TM, "https://www.agrocam.eu/product-page/agrocam-pro-rgb (accessed Oct 10, 2018)," [Online].

[30] T. N. C. J. P. J. D. C. D. Derave W, "Treadmill exercise negatively affects visual contribution to static postural stability," *International journal of sports medicine. 2002 Jan;23(01):44-9.*

[31] A. M. Al-Khazali HA, "Geometrical and graphical representations analysis of lissajous figures in rotor dynamic system," *IOSR Journal of Engineering,* vol. 2, no. 5, pp. 971-8, 2012.

[32] C. C. M. O. Minetti AE, "The mathematical description of the body centre of mass 3D path in human and animal locomotion," *Journal of biomechanics,* vol. 44, no. 8, pp. 1471-7, 2011 .

[33] K. M. B. G. R. H. Sandhya R, "Synthesis and analysis of geared five bar mechanism for ornithopter applications," in *Second International and 17th National Conference on Machines and Mechanism* , Kanpur, pp. 16-19, Dec 2015.

[34] S. A. El Menzhi L, "Lissajous Curve of an Auxiliary Winding Voltage Park Components for Doubly-Fed Induction Machine Electrical Faults Diagnosis," *Advanced Materials Research, Trans Tech Publications,* vol. 860, pp. 2223-2231, 2014.

[35] T. S. K. Jong-Won Kim, "A new design methodology for four-bar linkage mechanisms

based on derivations of coupler curve," *Mechanism and Machine Theory 100 (2016) 138–154.*

[36] M. K. D. H. K. R. Sandhya R, "Synthesis and Analysis of Geared Five Bar Mechanism for Ornithopter Applications," in *2nd International and 17th National Conference on Machines and Mechanisms.*

[37] A. N. M. Y. T. M. S. Bellakehal, "Force/position control of parallel robots using exteroceptive pose measurements," *Meccanica,* vol. 46, no. 1, pp. 195-205, Feb 2011 .

[38] S. J. Á. L. R. F. C. R. Traslosheros A, "Visual servoing for the Robotenis system: A strategy for a 3 DOF parallel robot to hit a Ping-Pong ball," in *2011 50th IEEE Conference on Decision and Control and European Control Conference*, 2011.

[39] M. M. Janabi-Sharifi F, "A kalman-filter-based method for pose estimation in visual servoing," *IEEE transactions on Robotics,* vol. 26, no. 5, pp. 939-47, 2010.

[40] I. E. R. E. U. O. G. J. Hernández L, "Kinematic task space control scheme for 3dof pneumatic parallel robot," *Intelligent Mechatronics,* pp. 67-84, 2011.

[41] M. M. K. A. M. M. K. N. Hesar ME, "Ball tracking with a 2-DOF spherical parallel robot based on visual servoing controllers," in *second RSI/ISM international conference on robotics and mechatronics (ICRoM),* 2014 Oct.

[42] J. N. C. M. S. &. N. I. Bouchrika, "Towards automated visual surveillance using gait for identity recognition and tracking across multiple non-intersecting cameras," *Multimedia Tools and Applications, vol. 75, pp. 1201-1221, Jan 2016 .*

[43] a. A. R. Z. K. Soomro, "Action recognition in realistic sports videos," *Computer vision in sports, Springer, pp. 181-208, 2014.*

[44] A. M. e. al, "Addition of a non-immersive virtual reality component to treadmill training to reduce fall risk in older adults (V-TIME): a randomised controlled trial," *The Lancet, vol. 338, pp. 1170-1182, Sep 2016.*

[45] M. E. e. al, "Learning multiple collaborative tasks with a mixture of interaction primitives," in *IEEE International Conference on Robotics and Automation (ICRA), 2015, pp. 1535-1542*.

[46] R. C. P. M. a. J. B. Joao F. Henriques, "High-Speed Tracking with Kernelized Correlation Filters," *IEEE Transactions on Pattern Analysis and Machine Intelligence* , vol. 37, no. 3, pp. 583-596, 2015.

[47] M. S. M.-C. F. J. D.-P. a. M. M.-Z. Pedraza-Hueso, "Rehabilitation using kinect-based games and virtual reality".

[48] F. M. A. a. W. F. B. Anderson, "Lean on Wii: physical rehabilitation with virtual reality Wii peripherals".

[49] C. M. H. J. M. M. D. D. B. T. P. A. T. L. Hannuna S, "Ds-kcf: a real-time tracker for rgb-d data," *Journal of Real-Time Image Processing. 2016 Nov:1-20.*.

[50] W. G. Y. Q. Liu T, "Real-time part-based visual tracking via adaptive correlation filters," in *InProceedings of the IEEE Conference on Computer Vision and Pattern Recognition 2015 (pp. 4902-4912).*.